

1 **Establishment of a pig influenza challenge model for evaluation of**
2 **monoclonal antibody delivery platforms**

3
4
5 Adam McNee^{1,8}, Trevor Smith^{2,8}, Barbara Holzer^{1,8}, Becky Clark¹, Emily Bessell¹,
6 Ghiabe Guibinga², Heather Brown², Katherine Schultheis², Paul Fisher², Stephanie
7 Ramos², Alejandro Nunez³, Matthieu Bernard³, Veronica Martini¹, Tiphany Chron¹,
8 Yongli Xiao⁴, John C. Kash⁴, Jeffery K. Taubenberger⁴, Sarah Elliott⁵, Ami Patel⁵,
9 Peter Beverley⁶, Pramila Rijal⁷, David Weiner⁵, Alain Townsend⁷, Kate Broderick^{2,8*}
10 and Elma Tchilian^{1,8*}

11
12
13 ¹ The Pirbright Institute, Pirbright GU24 0NF, UK

14 ² Inovio Pharmaceuticals, San Diego, CA 92121, USA

15 ³ APHA-Weybridge, New Haw, Addlestone, KT15 3NB, UK

16 ⁴ Viral Pathogenesis and Evolution Section, Laboratory of Infectious Diseases,
17 National Institute of Allergy and Infectious Diseases, National Institutes of Health,
18 Bethesda, MD 20892-3203 USA

19 ⁵ The Wistar Institute, Vaccine and Immunotherapy Center, Philadelphia, PA 19103,
20 USA

21 ⁶ National Heart and Lung Institute, St Mary's Campus, Imperial College London W2
22 1PG, UK

23 ⁷ Weatherall Institute of Molecular Medicine, University of Oxford, Oxford OX3 9DS,
24 UK

25
26 ⁸ These authors contributed equally

27
28 *Corresponding authors: kate.broderick@inovio.com and
29 elma.tchilian@pirbright.ac.uk

30

31 **Abstract**

32 Monoclonal antibodies are a possible adjunct to vaccination and drugs in treatment of
33 influenza virus infection. However questions remain whether small animal models
34 accurately predict efficacy in humans. We have established the pig, a large natural
35 host animal for influenza, with many physiological similarities to humans, as a robust
36 model for testing monoclonal antibodies. We show that a strongly neutralizing
37 monoclonal antibody (2-12C) against the hemagglutinin head administered
38 prophylactically at 15 mg/kg reduced viral load and lung pathology after pandemic
39 H1N1 influenza challenge. A lower dose of 1 mg/kg of 2-12C or a DNA plasmid
40 encoded version of 2-12C, reduced pathology and viral load in the lungs, but not viral
41 shedding in nasal swabs. We propose that the pig influenza model will be useful for
42 testing candidate monoclonal antibodies and emerging delivery platforms prior to
43 human trials.

44 Influenza virus infection remains a significant global health threat to humans and
45 livestock causing substantial mortality and morbidity. Monoclonal antibodies (mAbs)
46 administered either prophylactically or therapeutically have been proposed as a
47 strategy to provide immediate immunity and augment existing vaccines and drugs in
48 combatting seasonal and pandemic influenza infection. Broadly neutralizing
49 antibodies against conserved epitopes of the haemagglutinin (HA) stem and head,
50 and antibodies against the neuraminidase (NA) are candidates for human treatment
51 ^{1,2}. Both prophylactic and therapeutic administration of these antibodies have been
52 shown to be effective in the mouse and ferret³⁻¹⁰. However, early results from human
53 clinical trials showed that efficacy in mice and ferrets is not always predictive of
54 outcome in humans¹¹⁻¹⁴. The reasons for the apparent lack of efficacy in humans are
55 not clear but may include the difficulty of achieving high serum and nasal concentration
56 in a large body mass, the potency of the mAbs or the challenge of therapeutic
57 administration in the face of a high viral load. Variability due to pre-existing immunity
58 in human experimental or natural infection challenge studies is an additional problem.
59 There is therefore a need for a large animal model in which mAbs selected on the
60 basis of *in vitro* assays and efficacy in small animals can be further studied to help in
61 selecting promising mAbs and determining how best to administer them in clinical
62 trials. Pigs may provide such a model. They are large animals and a natural host for
63 influenza viruses. Pigs and humans are infected by the same subtypes of virus, have
64 the same distribution of sialic acid receptors in their respiratory tract and are
65 physiologically, anatomically and immunologically more similar to humans than small
66 animals^{15,16}.

67 While great progress in antibody delivery is being made, the high costs that are
68 associated with the production, purification and quality control are major challenges in

69 the development of clinical mAbs against influenza and other infectious diseases.
70 Moreover, long-term protection is difficult with a single inoculation because of the short
71 half-life of the mAb. Alternative *in vivo* antibody gene transfer strategies using DNA,
72 RNA or viral vectors have shown that antibody genes can be stably maintained in the
73 host tissue, resulting in potent and long-term expression of mAbs in the body following
74 a single administration¹⁷⁻²³. DNA plasmid encoded mAbs (dMAbs), which are delivered
75 to muscle tissue, are a novel approach with the potential to provide durable immunity²⁴⁻
76 ²⁶. The plasmid DNA is well-tolerated and nonintegrating, does not require cold-chain
77 distribution, can be delivered repeatedly and is relatively inexpensive to produce.
78 Previous studies have demonstrated the efficacy of such an approach for protection
79 against influenza in mice ²⁷.

80 We have previously tested therapeutic administration of the broadly neutralizing
81 anti-stem FI6 antibody in the pig influenza model. This did not reduce viral load in
82 nasal swabs and bronchoalveolar lavage (BAL), although there was reduction of
83 pathology after aerosol delivery²⁸. Broadly neutralizing anti-stem mAbs are less potent
84 at direct viral neutralization as compared to anti-head antibodies and require Fc
85 receptor engagement for *in vivo* protection^{29,30}. We demonstrated that human IgG1
86 FI6 did not bind to pig Fc receptors, perhaps accounting for the weak effect. Therefore
87 to establish a more robust pig model we reasoned that a strongly neutralizing strain
88 specific anti-head HA mAb should overcome this problem and give clear protection,
89 providing a benchmark against which other mAbs and delivery platforms might be
90 tested. Here we used the 2-12C mAb isolated from an H1N1pdm09 exposed
91 individual, which shows strong neutralizing activity and selects influenza virus variants
92 with HA substitutions K130E³¹. Furthermore we administered 2-12C prophylactically
93 to provide the best chance to reveal an effect on viral load, as it is challenging for

94 therapeutic administration to reduce viral load after infection has been established.
95 We went on to evaluate the potential of an *in vivo* produced 2-12C using synthetic
96 dMAb technology in support of the translation of this technology to humans as an
97 immunoprophylactic.

98

99 **Results:**

100 **Establishment of a prophylactic pig influenza challenge model with recombinant**
101 **2-12C mAb.** To establish a positive control protective mAb and delivery method in the
102 pig influenza model we tested the strongly neutralizing human IgG1 anti-head 2-12C
103 mAb³¹ in a prophylactic experiment. We administered 15 mg/kg of 2-12C intravenously
104 and the control groups received an isotype matched IgG1 mAb or the diluent. Twenty-
105 four hours later the pigs were challenged with pandemic swine H1N1 isolate,
106 A/swine/England/1353/2009 (pH1N1) and 4 days later culled to assess viral load and
107 pathology (**Fig. 1a**). 2-12C significantly decreased viral load in nasals swabs on each
108 day over the course of infection, although the decrease was less on days 2 and 3 than
109 days 1 and 4 (**Fig. 1b**). The total viral load in nasal swabs over the 4 days in animals
110 treated with 2-12C was also significantly less as determined by the area under the
111 curve (AUC) compared to diluent and isotype controls ($p=0.0267$ and $p=0.021$). Viral
112 load in the 2-12C group was significantly reduced in the BAL and no virus was detected
113 in the lungs at 4 days post infection (DPI). Overall 2-12C had a clear effect on viral
114 load in nasal swabs, BAL and lung.

115 The isotype and diluent control groups showed the most severe gross
116 pathology and histopathology scores (**Fig. 2a**). The red tan areas of pulmonary
117 consolidation were present mainly in the cranial and middle lung lobes of animals from
118 the isotype and diluent groups, but no lesions were found in the 2-12C group (**Fig. 2b**).

119 Similarly, necrotizing bronchiolitis and bronchial and alveolar exudation, and mild
120 thickening of the alveolar septa was shown in the animals from both control groups.
121 Minimal to mild alveolar septa thickening and lymphoplasmacytic peribronchial
122 infiltration was present in only one animal from the 2-12C treated group. Influenza A
123 nucleoprotein (NP) (brown labelling) was detected by immunohistochemistry (IHC) in
124 the bronchial and bronchiolar epithelial cells, alveolar cells and exudate in the
125 bronchioles and alveoli in both control groups. No NP labelling was found in the lung
126 of animals treated with 2-12C.

127 Recombinant 2-12C was detected in the serum at a mean concentration of 74.6
128 $\mu\text{g/ml}$ and in the BAL at 183.9 ng/ml at 4 DPI as determined by an HA ELISA (**Fig.**
129 **3a**). HA specific IgG was also detected in nasal swabs at a mean concentration of 24
130 ng/ml . The serum of the 2-12C treated group exhibited strong neutralizing activity at a
131 50% inhibition titer of 1:8,000 and 1:164 in the BAL (**Fig. 3b**). Neutralizing activity in
132 nasal swabs could not be tested due to limited sample availability. These data show
133 that prophylactic intravenous administration of recombinant 2-12C at 15 mg/kg
134 significantly reduced viral load and pathology in the pig, a large natural host animal.

135

136 **Design and expression of DNA encoded mAb (dMAb) in pigs and mice.** To
137 investigate the potential of a DNA-launched influenza mAb to mediate disease
138 protection in the pigs we designed and engineered dMAb 2-12C (**Fig. 4a**). The gene
139 sequences of the human IgG1 heavy and light chains were codon and RNA-optimized
140 and inserted into a single modified-pVax1 DNA expression vector plasmid, separated
141 by furin and P2A peptide cleavage sites. Expression of dMAb 2-12C was confirmed
142 by Western Blot analysis, the band was detected at the same molecular weight as rec
143 2-12C (**Fig. 4b**). To assess *in vivo* expression, dMAb 2-12C was formulated with

144 human recombinant hyaluronidase, as an optimization to enhance gene expression in
145 the context of delivery with adaptive *in vivo* electroporation³². We measured
146 expression of human IgG in myocytes 3 days after the administration of dMAb 2-12C
147 pDNA into the tibialis anterior muscle of BALB/c mice, confirming local expression of
148 human IgG at the site of delivery (**Fig. 4c**). To assess levels and durability of *in vivo*
149 expression, mice were conditioned to reduce the T cell compartment using CD4 and
150 CD8-depleting antibodies, this has been shown to permit the expression of a human
151 mAb construct in mice in the absence of a host anti-drug antibody (ADA) response²⁵.
152 Administration of dMAb 2-12C pDNA to the tibialis anterior muscle was associated an
153 increased durability of circulating levels of the mAb in the serum compared to rec 2-
154 12C, administered intravenously (**Fig. 4d**).

155 *In vivo* expression of dMAb 2-12C was measured in pigs. Expression of human
156 IgG in myocytes 3 days after the administration of dMAb 2-12C pDNA into the
157 quadriceps muscle of the pig, confirmed the local expression of the human IgG at the
158 site of delivery (**Fig. 5a**). We measured serum levels of the expressed mAb after the
159 day 0 administration of a total dose of 24 mg dMAb 2-12C pDNA into the quadriceps
160 of the pig. Circulating levels of the expressed mAb in the serum were detected by an
161 HA ELISA (**Fig. 5b**). Peak levels were 7 and 12 µg/ml for the two animals. Influenza
162 H1N1 neutralizing activity (1:640 peak activity in both pigs) of the serum harboring the
163 *in vivo* expressed 2-12C mAb was measured in a microneutralization assay (**Fig. 5c**).
164 In both pigs, reductions in the serum levels of the expressed mAb and serum
165 neutralizing activity were associated with the detection of an anti-drug antibody (ADA)
166 response against the human 2-12C mAb (**Fig. 5b-d**). These results demonstrate that
167 dMAb 2-12C induces expression of human 2-12C after intramuscular delivery by
168 electroporation in mice and pigs.

169

170 **Assessment of rec 2-12C dosing and dMAb 2-12C in a pig influenza model.** After
171 we had established 2-12C as a robust positive control antibody, we tested a lower
172 dose of rec 2-12C and the efficacy of dMAb 2-12C in the pig influenza challenge
173 model. The dMAb 2-12C was administered 6 days before the pH1N1 challenge to
174 allow for accumulation of the *in vivo* expressed 2-12C mAb in the host. Preliminary
175 experiments indicated the serum levels of 2-12C were generally not negatively
176 impacted by the ADA until day 9, so we believed this schedule allowed a window of 3-
177 4 days to test the efficacy of dMAb 2-12C. Recombinant 2-12C at 15 mg/kg and 1
178 mg/kg were delivered intravenously 24 hours before challenge to 6 pigs per group
179 **(Fig. 6a).**

180 As before, the greatest effect on virus replication in nasal swabs of 2-12C at 15
181 mg/kg was at day 1 and day 4 post infection, although no virus detected in BAL and
182 accessory lung lobe **(Fig. 6b)**. The AUC in the 2-12C group was significantly different
183 from the control ($p=0.0235$). The lower dose of 2-12C at 1 mg/kg did not have a
184 statistically significant effect on viral load in nasal swabs or BAL, although it reduced
185 the titer in the lung accessory lobe. Similarly, dMAb 2-12C did not have a significant
186 effect on viral load in nasal swabs or BAL, but significantly reduced viral load in lung.

187 The gross pathology was reduced in all experimental groups although this was
188 significant only in the rec mAb groups, due to an outlier score in one animal in the
189 dMAb 2-12C group. Histopathological evaluation also showed significantly decreased
190 scores in all experimental groups **(Fig. 7a, b)**. All animals from the control group
191 displayed changes consistent with a mild to moderate bronchointerstitial pneumonia,
192 with various degrees of lymphohistiocytic septal infiltration and bronchial and
193 perivascular cuffing, and with frequent areas of necrotizing and suppurative

194 bronchiolitis. Viral antigen was detected by IHC in bronchial and bronchiolar epithelial
195 cells, alveolar epithelial cells and exudate (macrophages) in all 6 control animals.
196 Milder changes, mainly located in the septa, were found in animals from the antibody
197 treated groups. The extent of bronchiolar changes and presence of IHC labelling
198 varied in each group, although at least one animal per group displayed bronchiolar
199 changes and virus antigen detection, in contrast to experiment 1. In addition to the
200 differences in the histopathological scores, rec 2-12C 15 mg/kg group had 2 animals
201 with acute bronchial lesions and antigen detection, whereas rec 2-12C 1 mg/kg group
202 had 3 animals with bronchial lesions and antigen. The dMAb group had 1 animal with
203 acute bronchial lesion and 5 animals where antigen was detected.

204 The concentration of the mAbs in the serum was determined daily after
205 challenge. 2-12C was detected in the 15 mg/kg group at 101 $\mu\text{g/ml}$ and in the 1 mg/kg
206 group at 10 $\mu\text{g/ml}$ 24 hours after administration. This declined in both groups over the
207 next 3 days (**Fig. 8a**). In contrast the dMAb reached its peak of 0.99 $\mu\text{g/ml}$ at day 7
208 after administration, declining thereafter. In the BAL HA specific antibodies were
209 detected in the rec 2-12C groups (mean of 320.3 ng/ml for the 2-12C 15 mg/kg and 8
210 ng/ml for the 1mg/kg 2-12C groups) and a trace in the dMAb (1.5 ng/ml). In nasal
211 swabs HA specific antibodies were detected in the 15mg/kg 2-12C group at 21.9 ng/ml
212 4DPI (**Fig. 8a**).

213 Neutralizing activity in serum was detected in all groups (**Fig. 8b**). There was
214 50% inhibition titer of 1: 14,600 for the 15 mg/kg group and 1:1,280 for the 1mg/kg
215 group at the time of challenge. A peak titer of 1:136 was detected at day 7 in the dMAb
216 2-12C-treated group. MN activity in BAL was only seen in the rec 2-12C 15 mg/kg
217 group. A pig anti-2-12C ADA response was detectable in the dMAb group at day 8
218 after administration increasing at day 10 (**Fig. 8c**). No ADA response was seen to the

219 rec proteins in the serum, most likely because the animals were culled only 4 days
220 after rec antibody administration.

221 Overall these results indicate that rec 2-12C offers robust protection at 15
222 mg/kg and that this correlates with mAb concentration and neutralization in serum.
223 Administration of recombinant 2-12C protein at 1 mg/kg and dMAb 2-12C at 6 mg (0.5
224 mg DNA/kg) significantly reduced lung pathology and viral load in the lungs, but not
225 in nasal swabs or BAL.

226

227 **Sequencing of virus.** Inoculant virus and viruses from nasal swab samples of two
228 control pigs and two 2-12C (15 mg/kg) treated pigs at 3 DPI were subjected to deep
229 sequence analysis. In the inoculant, two control samples, and one of the 2-12C treated
230 samples (53_2-12C), all segments of the influenza genome had 100% coverage with
231 lowest average per base coverage of 98384.7 for NA segment in sample of 53-2-12C.
232 For the other 2-12C treated sample (51_2-12C), the lowest segment coverage was
233 94.8% for the NA segment with average per base coverage of 2587.7. Although the
234 inoculant had been passed in MDCK cells for at least 5 times, from these sequencing
235 data, a total of only 5 SNPs (3 non-synonymous SNPs) were detected as compared
236 to the reference *A/swine/England/1353/2009* (pH1N1) sequence (Table 1). Non-
237 synonymous SNPs found in sequenced nasal swab samples of 2 control and two 2-
238 12C (15 mg/kg) treated pigs at 3 DPI compared to *A/swine/England/1353/2009* are
239 shown in Table 2. One non-synonymous SNP (HA K226E) that was detected in 2
240 control samples and one 2-12C treated sample (51_2-12C), was also identified as one
241 of the HA SNPs found in the inoculant virus (Table 1). Three non-synonymous SNPs
242 were detected in the other 2-12C treated sample (53_2-12C). One of them was also
243 HA K226E, while the other 2 SNPs (HA G172E and HA T201I) were not detected in

244 inoculant virus. Their frequencies in sample 53_2-12C are 12.1% (HA G172E) and
245 11.1% (HA T201I) respectively (Table 2). Therefore, from our deep sequencing data,
246 we did not see evidence of escape of virus from antibody 2-12C (15 mg/kg) at day 3.
247 No mutations in the 2-12C binding site were detected. Similarly no evidence for viral
248 evolution driven by 2-12C was detected in day 4 nasal swab samples in the 1mg /kg
249 and dMAb treated groups (data not shown).

250

251 **Discussion**

252 In the last decade there has been extensive research on the use of mAbs for passive
253 immunization against influenza. mAbs could be used as pre- or post-exposure
254 treatment to prevent or reduce severe disease. They have the advantage of providing
255 immediate immunity and bridging the gap between the start of a pandemic and vaccine
256 availability. In order to test candidate mAbs and delivery platforms, we have
257 established a reproducible and robust pig influenza challenge model and identified a
258 protective human HA1 specific mAb, 2-12C, which can be used as a standard to
259 benchmark other mAb candidates and delivery platforms. Both viral load and
260 pathology were significantly reduced when the recombinant 2-12C mAb was given at
261 15 mg/kg intravenously 24 hours before pH1N1 challenge. Furthermore, the mAb-
262 mediated a significant reduction in lung pathology upon administration at a lower dose
263 as a recombinant protein (1 mg/kg) or as a dMAb (0.5 mg DNA/kg). No evidence for
264 2-12C driven viral evolution was detected in any group. However, it is important to
265 reflect that 2-12C, which is a typical mAb to the globular head of HA, selects resistance
266 mutations *in vitro* at position K130^{31,33}. While the epitope recognized by 2-12C has
267 remained stable in circulating seasonal H1N1 viruses for ten years, in 2019 viruses
268 have appeared with a substitution at N129D in the haemagglutinin that are resistant

269 to neutralization by 2-12C (Rijal unpublished, Crick Reports September 2019,
270 [https://www.crick.ac.uk/partnerships/worldwide-influenza-centre/annual-and-interim-](https://www.crick.ac.uk/partnerships/worldwide-influenza-centre/annual-and-interim-reports)
271 [reports](https://www.crick.ac.uk/partnerships/worldwide-influenza-centre/annual-and-interim-reports)). While antibodies to the globular head are profoundly protective, they will need
272 to be regularly updated.

273 Conventional mAbs remain an expensive approach from a manufacturing
274 perspective so that a simple, cost-effective passive immunization strategy inducing
275 sustained *in vivo* production would be extremely valuable. dMAbs, a DNA plasmid
276 encoding mAbs have the potential to circumvent cost constraints and provide durable
277 immunity, perhaps for the duration of an influenza pandemic or season²⁴⁻²⁷. Here we
278 tested 2-12C dMAb in the pig influenza model and although the serum concentration
279 of *in vivo* expressed dMAb was 100 times lower (~1 µg/ml) than in pigs given the
280 recombinant protein at 15 mg/kg (~100 µg/ml) we observed significant protection
281 against disease pathology in the lungs. This was encouraging as a relatively low dose
282 of dMAb was used (0.5 mg DNA/kg), and the anti-human 2-12C response induced in
283 the pig prevented peak concentration from being achieved (Fig. 5 and 6).

284 We also tested 2-12C dMAb, partially porcised with pig Fc IgG3, and
285 observed similar protection and an ADA response (data not shown), indicating that the
286 human Fab still induces an antibody response. Figure 4d exemplifies a typical PK
287 curve in the absence of an ADA. Using pig influenza-specific antibodies will circumvent
288 this problem. We have generated a number of high affinity pig influenza neutralizing
289 antibodies which will provide a more relevant test system to evaluate delivery of novel
290 dMAbs and other emerging platforms in pigs. Furthermore these porcine mAbs will
291 allow detailed investigation of pharmacokinetics and protective mechanisms in a
292 relevant natural host large animal model.

293 A number of outstanding questions remain for mAb therapy and this pig model
294 will provide an opportunity to investigate them. We still do not know the minimal
295 protective dose of 2-12C since 15 mg/kg reduced both viral load and pathology, while
296 1 mg/kg reduced only pathology. In the rec 2-12C 15 mg/kg group 2-12C was detected
297 in the BAL (320 ng/ml), in the 1 mg/kg group (8 ng/ml) and in the dMAb group (1.4
298 ng/ml), suggesting that it does reach mucosal surfaces although virus neutralization
299 and reduction of BAL viral load was only observed in the 15 mg/kg group. In the 15
300 mg/kg group only 2-12C was detected in nasal swabs at 4 DPI, perhaps because of
301 competition with the virus. However it remains to be determined whether reduction in
302 viral load or gross and histo-pathology better correlate with disease morbidity and
303 mortality. In this pig model, pH1N1 causes only a mild disease and neither moderate
304 nor severe clinical signs were detected in any animal. However other influenza viruses,
305 which cause more severe clinical signs in pigs would enable us to determine whether
306 reduction of pathology without reduction in viral load correlates with symptom
307 reduction. Studies on alternative biomarkers such as gene signatures or cytokines
308 during mAb treatment may provide novel methods for predicting success or failure.

309 Here we tested the effect of prophylactic 2-12C before a high viral load is
310 established as would be the case with therapeutic administration. However we still
311 inoculate the pigs with a very high dose of virus and it would be important to test the
312 effect of mAbs in a contact challenge model which more closely mimics natural
313 infection.

314 In our previous studies we used the human broadly neutralizing anti-stem FI6
315 mAb and showed only marginal protective effect on gross pathology after aerosol
316 delivery. We were unable to detect binding of FI6 to porcine PBMC or ADCC when
317 porcine PBMC were used. More refined analysis of binding of human IgG to the

318 Göttingen minipig Fc gamma receptors (FcγR) indicated that the binding affinities for
319 human IgG to porcine FcγRIa, FcγRIIa and FcγRIIb were comparable to the respective
320 human FcγRs³⁴. However there was no binding of hu IgG1 to the poFcγRIIIa, which is
321 an important mediator of ADCC in monocytes and natural killer cells. The lack of
322 binding to porcine poFcγRIIIa may abrogate or greatly reduce Fc-mediated functions
323 of human mAbs in agreement with our previous study²⁸. This data suggest that there
324 is a need for further investigation of which Fc receptors, Ig classes and subclasses are
325 critical for therapeutic effects of mAbs *in vivo*.

326 An essential component in development of mAbs therapies is the need to
327 improve existing animal models to more closely mimic humans. Unfortunately, all
328 animal models have limitations in recapitulating the full range of disease observed in
329 humans. Mice, guinea pigs, ferrets and non-human primates (NHP) are used for
330 influenza-virus research, with the ferret considered to represent the "gold standard".
331 However mice cannot be infected with most strains of the influenza virus and do not
332 recapitulate signs of illness observed in humans, guinea pigs do not exhibit overt signs
333 of illness and ferrets may have different drug pharmacokinetics to humans³⁵⁻³⁸.
334 NHPs share many physiological and genetic similarities to humans and are naturally
335 susceptible to influenza virus infection, however there are ethical considerations, they
336 are costly, not easily accessible, and generally weigh as little as 2-4 kg. In contrast,
337 the pig is a large animal and a natural host for the same subtypes as human seasonal
338 strains as well as a source of new human pandemic viruses¹⁶. Our pigs were between
339 11-14 kg, but pigs with equivalent weights to humans are available. A further
340 advantage of the pig model is that the same pdmH1N1 virus circulates in both pigs
341 and humans and has been used in human challenges as well as in our pig model³⁹⁻

342 41. Therefore findings in the pig could be directly tested in humans to further validate
343 the model.

344 In summary we have established a positive control protective influenza mAb
345 and delivery method to benchmark mAb delivery platforms. This will enable testing of
346 further improvements in the mAb delivery platforms, the effect of therapeutic
347 administration and whether cocktails of mAbs will provide synergy by harnessing both
348 classical neutralization and Fc mediated effector mechanisms. Furthermore, research
349 in the pig has the additional benefit in facilitating development of new platforms for
350 interventions in livestock diseases. We propose that the pig influenza model will
351 become a critical tool to accelerate mAb development to the clinic by validating lead
352 mAbs from smaller animal models and evaluating emerging delivery approaches.

353

354 **Materials and methods**

355 **Antibody preparation.** The anti-influenza human IgG1 mAb 2-12C and the anti-
356 fluorescein human IgG1 isotype control were produced in bulk by Absolute Antibody
357 Ltd (Redcar, UK). They were dissolved in 25mM Histidine, 150 mM NaCl, 0.02%
358 Tween, pH6.0 diluent. We also engineered synthetic plasmid DNA to encode the
359 human 2-12C. A single plasmid was designed to encode both the mAb 2-12C heavy
360 and light chains under the control of a human CMV promoter and human IgG signal
361 sequence and bovine growth hormone polyadenylation signal. The heavy and light Ig
362 chains genes were separated by both a furin cleavage and a P2A cleavage site to
363 ensure complete processing of the two proteins. The resulting construct was named
364 dMAb 2-12C.

365

366 **Influenza challenge studies in pigs.** All experiments were approved by the ethical
367 review processes at the Pirbright Institute and Animal and Plant Health Agency
368 (APHA) and conducted according to the UK Government Animal (Scientific
369 Procedures) Act 1986. APHA conforms to ARRIVE guidelines. Two pig influenza
370 challenge experiments were carried out.

371 For the first experiment, fifteen 5 weeks old Landrace x Hampshire cross,
372 female pigs were obtained from a commercial high health status herd and were
373 screened for absence of influenza A infection by matrix gene real time RT-PCR and
374 for antibody-free status by hemagglutination inhibition using four swine influenza virus
375 antigens – pdmH1N1, H1N2, H3N2 and avian-like H1N1. Pigs weighed between 11
376 and 14 kg (average 12.5 kg). Pigs were randomized
377 (<https://www.graphpad.com/quickcalcs/randomize1/>) into three groups of five animals as
378 follows: the first control group received 1 ml/kg histidine diluent only; the second
379 isotype control group received 15 mg/kg anti-fluorescein IgG1 mAb intravenously and
380 the third 2-12C group received 15mg/kg 2-12C intravenously. The antibodies were
381 administered to the ear vein of animals sedated with stesnil. Twenty four hours after
382 mAb administration all animals were challenged intranasally with 3×10^6 PFU of
383 pandemic swine H1N1 isolate, A/swine/England/1353/2009 (pH1N1) in 4 ml (2ml per
384 nostril) using a mucosal atomization device MAD300 (Wolfe Tory Medical).

385 In the second challenge experiment thirty, 5 weeks old Landrace x Hampshire
386 cross, influenza free female pigs were obtained and their influenza free status
387 confirmed as above. The weights of the pigs were between 12 and 14 kg (average of
388 12.9 kg). The pigs were randomized into 4 groups of 6 as follows: control untreated;
389 15 mg/kg recombinant 2-12C intravenously; 1 mg/kg recombinant 2-12C intravenously
390 and the final group received 6 mg human dMAb 2-12C. Recombinant 2-12C protein

391 was administered intravenously 24 hours before the pH1N1 challenge to sedated pigs
392 and dMAbs were administered by electroporation to pigs sedated with 4mg/kg Zoletil
393 and 0.04 mg/kg Domitor, 6 days before the pH1N1 influenza challenge. Six mg of
394 dMAb 2-12C pDNA was formulated with 135 U/ml Hylenex (Halozyme, CA), the
395 formulation was administered intramuscularly to the back left quadriceps of the animal,
396 and followed by *in vivo* electroporation using the CELLECTRA® constant current
397 device. All animals were challenged with 3.4×10^6 PFU pH1N1 in 4ml (2ml per nostril)
398 using MAD. Clinical signs (temperature, state of breathing, coughing, nasal discharge,
399 appetite, altered behavior) observed were mild and none of the pigs developed
400 moderate or severe disease.

401

402 **Pathological and histopathological examination of lungs.** Animals were humanely
403 killed four days post infection (DPI) with an overdose of pentobarbital sodium
404 anesthetic. The lungs were removed and digital photographs taken of the dorsal and
405 ventral aspects. Macroscopic pathology was scored blind as previously reported⁴².
406 The percentage of the lung displaying gross lesions for each animal was calculated
407 using image analysis software (Fiji ImageJ) on the digital photographs. Lung tissue
408 samples from cranial, middle and caudal lung lobes were taken from the left lung and
409 collected into 10% neutral buffered formalin for routine histological processing.
410 Formalin fixed tissues were paraffin wax-embedded and 4- μ m sections cut and
411 routinely stained with hematoxylin and eosin (H&E). Immunohistochemical detection
412 of influenza A virus nucleoprotein was performed in 4- μ m tissue sections as previously
413 described⁴³. Histopathological changes in the stained lung tissue sections were scored
414 by a veterinary pathologist blinded to the treatment group. Lung histopathology was
415 scored using five parameters (necrosis of the bronchiolar epithelium, airway

416 inflammation, perivascular/bronchiolar cuffing, alveolar exudates and septal
417 inflammation) scored on a 5-point scale of 0 to 4 and then summed to give a total slide
418 score ranging from 0 to 20 per slide and a total animal score from 0 to 60⁴⁴. The slides
419 were also scored using the “Iowa” method, that also takes into account the amount of
420 viral antigen present in the sample, as described⁴⁵.

421
422 **Tissue sample processing.** Four nasal swabs (NS) (two per nostril) were taken at 0,
423 1, 2, 3, 4 DPI. The swabs were placed into 1 ml of Trizol or 2 ml of virus transport medium
424 comprising tissue culture medium 199 (Sigma-Aldrich) supplemented with 25mM
425 HEPES, 0.035% sodium bicarbonate, 0.5% bovine serum albumin (BSA), penicillin 100
426 IU/ml, streptomycin 100 µg/ml and nystatin 0.25 µg/ml, vortexed, centrifuged to remove
427 debris and stored at -80°C for subsequent virus titration. Blood samples were collected
428 at the start of the study (prior to antibody administration) and at the indicated times post
429 mAb delivery and challenge. Broncho-alveolar lavage (BAL) was collected from the
430 entire left lung with 150ml of virus transport medium (described above). BAL samples
431 were centrifuged at 300 x g for 15 minutes, supernatant was removed, aliquoted and
432 frozen for antibody analysis.

433
434 **Virus titration and viral RNA isolation.** Viral titers in nasal swabs, BAL and
435 accessory lung lobe were determined by plaque assay on MDCK cells (Central Service
436 Unit, The Pirbright Institute, UK). Samples were 10-fold serially diluted in Dulbecco’s
437 Modified Eagle’s Medium (DMEM) and 100µl overlaid on confluent MDCK cells in
438 12 well tissue culture plates. After 1 hour, the plates were washed and overlaid with
439 2ml of 0.66 % agarose containing culture medium. Plates were incubated at 37°C for
440 48 to 72 hours and plaques visualized using 0.1% crystal violet. For sequencing nasal

441 swabs were collected in 1 ml of Trizol (Invitrogen, Thermo Fisher Scientific, UK) and
442 RNA was extracted by chloroform and isopropanol precipitation.

443

444 **Next generation sequencing.** Viral RNA enriched library production and viral cDNA
445 library sequencing were as previously reported⁴⁶. Briefly, isolated RNA was amplified
446 using the Ovation RNA-Seq system V2 from NuGEN (NuGEN, San Carlos, CA). The
447 amplified total cDNAs were analyzed by an Agilent 2100 Bioanalyzer using the Agilent
448 High Sensitivity DNA Kit (Agilent Technologies, Santa Clara, CA) and sheared to
449 150bp on the Covaris S2 machine (Covaris, Woburn, MA). Approximately 400 ng of
450 amplified cDNA was used to generate the Illumina sequencing library using the Agilent
451 SureSelectXT Target Enrichment Kit (Agilent, Santa Clara, CA) for Illumina Multiplex
452 Sequencing by using enrichment probes designed for A/California/04/2009(H1N1)
453 virus. Enriched Illumina sequencing libraries were sequenced on an Illumina NextSeq
454 sequencer (Illumina, San Diego, CA).

455

456 **Data analysis.** Reads were mapped to the HISAT2 indexed
457 A/swine/England/1353/2009 (pH1N1) genome using HISAT2 (release 2.0.5,
458 <https://ccb.jhu.edu/software/hisat2/index.shtml>) downloaded from the Center for
459 Computational Biology, Johns Hopkins University⁴⁷. SAMtools mpileup (version
460 2.1.0)⁴⁸ was used to make SNP calls with minimum base Phred quality score as 25.
461 A reported SNP call was one that satisfied the following criteria at the SNP position:
462 1) more than 100 reads at that position⁴⁹⁻⁵¹ 2) reads present from both directions, 3)
463 variant calls exactly at the end of the read eliminated and 4) reads with bases that are
464 different to reference more than 10% of the aligned reads.

465

466 **Microneutralization assay.** Neutralizing Ab titers were determined in serum and BAL
467 fluid using a microneutralization (MN) assay as previously described⁵². In brief, pig
468 sera or BAL fluid were heat-treated for 30 min at 56°C and diluted 1:10 for serum and
469 1:2 for BAL as a starting point for the assay. Fifty µl of serially diluted samples were
470 incubated with an equal volume of pH1N1 (the virus was titered beforehand in the
471 absence of serum to determine the PFU/ml necessary to yield a plateau infection in
472 the MN assay). After 2h MDCK SIAT-1 cells at 3×10^4 cells/well were added to the
473 serum/virus and incubated for 18 h. The fixed and permeabilized cell monolayer was
474 stained with anti-nucleoprotein (Clone: AA5H, Bio-Rad Antibodies, UK) followed by
475 goat anti-mouse HRP (DAKO) antibody. After addition of the 3,3',5,5'-
476 tetramethylbenzidine (TMB) substrate the reaction was stopped with 1M sulfuric acid
477 and absorbance was measured at 450 nm and 570 nm (reference wavelength) on the
478 Cytation3 Imaging Reader (Biotek). The MN titers were expressed as half maximal
479 inhibitory dilution (50% Inhibitory titer is: midpoint between uninfected control wells
480 and virus-infected positive controls) derived by linear interpolation from neighbouring
481 points in the titration curve.

482

483 **Enzyme-linked immunosorbent assays (ELISA).** Antibody titers against the pH1N1
484 HA in the serum, BAL fluid and nasal swabs were determined by ELISA. The
485 recombinant HA protein of A/Eng/195/2009 containing a C-terminal thrombin cleavage
486 site, a trimerization sequence, a hexahistidine tag and a BirA recognition sequence
487 was expressed in HEK293 cells and purified as described previously⁵². Ninety six-well
488 microtiter plates (Maxi Sorp, Nunc, Sigma-Aldrich, UK) were coated with 50 µL
489 recombinant protein at a concentration of 1 µg/mL in carbonate buffer overnight at
490 4 °C. Plates were blocked with 200 µl blocking solution of 4% milk powder in PBS,

491 supplemented with 0.05% Tween-20 (PBS-T) for 2 h at room temperature. Samples
492 were serially diluted in PBS-T with 4% milk powder and added to the wells for 1h on a
493 rocking platform. The plates were washed three times with PBS-T and 100 μ l of
494 horseradish peroxidase (HRP)-conjugated goat anti-human or goat anti-pig Fc
495 fragment secondary antibody (Bethyl Laboratories) diluted in PBS-T with 4% milk
496 powder was added and plates incubated for 1 h at room temperature. The plates were
497 washed four times with PBS-T and developed with 100 μ L/well TMB High Sensitivity
498 substrate solution (BioLegend, UK). After 5 to 10 min the reaction was stopped with
499 100 μ L 1M sulfuric acid and the plates were read at 450 and 570 nm with the Cytation3
500 Imaging Reader (Biotek). A standard curve was generated using rec 2-12C antibody
501 (Absolute Antibody). The data were analyzed in Microsoft Excel and GraphPad Prism.
502 The cut off value was defined as the average of all blank wells plus three times the
503 standard deviation of the blank wells.

504 For detection of an antibody response to 2-12C in pigs (ADA), ninety six-well
505 microtiter plates (Maxi Sorp, Nunc, Sigma-Aldrich) were coated with 2 μ g/ml rec 2-12C
506 (Absolute Antibody) in PBS-T overnight at 4°C. The plates were washed and blocked.
507 Pre-diluted serum samples in T-PBS were added and incubated for 2h at room
508 temperature. The plates were washed 3 times and goat anti-pig H+L-HRP (Bethyl
509 Laboratories) was added for 1 h at room temperature and developed as above.

510

511 ***In vitro* transfection of dMAb 2-12C.** Lipofectamine 3000 transfection kit
512 (ThermoFisher, Waltham, MA) was used to transfect adherent HEK 293T cells
513 (ATCC® CRL11268™) with dAMB 2-12C plasmids. Medium was harvested 72 h post
514 transfection and filtered using 0.22 μ m stericup-GP vacuum filtration system (Millipore,
515 Burlington, MA). The supernatant from pDNA transfected cells was purified using

516 Protein G GraviTrap (GE Healthcare, Chicago, IL) according to the manufacturer's
517 instructions. The eluted protein was concentrated by Amicon Ultra-15 Centrifugal Filter
518 unit (30 kDa) and quantified by nanodrop.

519

520 **Western blot.** 0.5 µg of each sample was loaded on a NuPAGE™ 4-12% Bis-Tris gel
521 (ThermoFisher). Precision Plus Protein Kaleidoscope Prestained Protein Standard
522 (Bio-Rad, Hercules, CA) was used as the standard marker. The gel was transferred to
523 a PVDF membrane using iBlot™ 2 Transfer device (Invitrogen, Waltham, MA). The
524 membrane was blocked with goat histology buffer (1% BSA (Sigma, St. Louis, MO),
525 2% goat serum (Sigma), 0.3% Triton-X (Sigma) and 0.025% 1g/ml Sodium Azide
526 (Sigma) in PBS) for 30 minutes at room temperature. Goat anti-human IgG-Fc
527 fragment antibody (A80-104A, Bethyl, Montgomery, TX) diluted in 1:1000 in goat
528 histology buffer was added and incubated for 1 hour at room temperature. After
529 washing the blot for 5 minutes in DPBS (HyClone, Logan, UT) three times, donkey
530 anti-goat IgG HRP antibody (Abcam, Cambridge, UK) in 1:2000 dilution in goat
531 histology buffer was added and incubated for 1 hour at room temperature. After
532 washing the blot three times for 5 minutes in DPBS, the membrane was developed
533 using ECL™ Prime Western Blotting system (GE Healthcare) and imaged using
534 Protein Simple FluorChem System.

535

536 ***In vivo* dMAb 2-12C mouse and pig immunogenicity and pharmacokinetic**
537 **studies.** Female BALB/c mice between 4 and 6 weeks of age were group-housed with
538 *ad libitum* access to feed and water. Husbandry was provided by Acculab (San Diego,
539 CA) and all procedures were in compliance with the standards and protocols of the
540 Institutional Animal Care and Use Committee (IACUC) at Acculab. To deplete T cell

541 populations BALB/c mice received one intraperitoneal injection of 500 µg of anti-
542 mouse CD4 (BE0003-1, BioXCell, West Lebanon, NH) and 500 µg of anti-mouse
543 CD8α (BioXCell, BE0117) in 300 µl of PBS. 200 µg dMAb plasmid DNA was
544 formulated with 135 U/ml of human recombinant hyaluronidase (Hylenex®, Halozyme,
545 San Diego, CA). Mice received an intramuscular (IM) administration of formulation
546 followed by electroporation (EP). EP was delivered at the injection site with the
547 CELLECTRA-3P® adaptive *in vivo* electroporation system. An array of three needle
548 electrodes with 3 mm insertion depth was used. The EP treatment consists of two sets
549 of pulses with 0.1 Amp constant current with the second pulse set delayed by 3
550 seconds. Within each set there are two 52 ms pulses with a 198 ms delay between
551 the pulses. 100 µl recombinant 2-12C was injected intravenously (IV) at a dose of 1
552 mg/kg.

553 Pigs received intramuscular administration of up to 24 mg of dMAb plasmid
554 DNA formulated with 135 U/ml of human recombinant hyaluronidase. EP was
555 delivered at the injection site with the CELLECTRA-5P® adaptive *in vivo*
556 electroporation system. For pharmacokinetic (PK) studies, blood samples were drawn
557 at the indicated time points.

558

559 **Immunofluorescence staining and imaging.** *In vivo* expressed 2-12C: 3 days after
560 IM delivery of dMAb 2-12C pDNA, mouse and pig muscle tissues were harvested,
561 fixed in 10% Neutral-buffered Formalin (BBC Biochemical, Stanford, MA) and
562 immersed in 30% sucrose (Sigma) in deionised water for *in vivo* staining of dMAb
563 expression. Tissues were then embedded into O.C.T. compound (Sakura Finetek,
564 Torrance, CA) and snap-frozen. Frozen tissue blocks were sectioned to a thickness of
565 18 µm. Slides were incubated with Blocking-Buffer (0.3% Triton-X (Sigma), 2% donkey

566 serum in PBS) for 30 min, covered with Parafilm. Goat anti-human IgG-Fc antibody
567 (Bethyl) was diluted 1:100 in incubation buffer (1% BSA (Sigma), 2% donkey serum,
568 0.3% Triton-X (Sigma) and 0.025% 1g/ml Sodium Azide (Sigma) in PBS). 150 µl of
569 staining solution was added to each slide and incubated for 2 hrs. Slides were washed
570 in PBS three times. Donkey anti-goat IgG AF488 (Abcam, Cambridge, UK) was diluted
571 1:200 in incubation buffer and 50 µl was added to each section. Slides were washed
572 after 1hr incubation and mounted with DAPI-Fluoromount (SouthernBiotech,
573 Birmingham, AL) and covered. Slides were imaged with a BX51 Fluorescent
574 microscope (Olympus, Center Valley, PA) equipped with Retiga3000 monochromatic
575 camera (QImaging, Surrey, Canada).

576

577 **Quantification of human IgG in dMAb 2-12C treated animals.** 96-well assay plates
578 (Thermo Scientific) were coated with 1 µg/well goat anti-human IgG-Fc fragment
579 antibody (Bethyl) in DPBS (ThermoFisher) overnight at 4°C. Next day plates were
580 washed with 0.2% Tween-20 in PBS and blocked with 10% FBS in DPBS for 1hr at
581 room temperature. The serum samples were diluted in 1% FBS in 0.2% Tween -PBS
582 and 100 µl of this mix was added to the washed assay plate. Additionally, a standard
583 curve of recombinant 2-12C mAb prepared as 1:2 serial dilutions, starting at 500 ng/ml
584 in dilution buffer and added in duplicate to each assay plate. Samples and standard
585 were incubated for 1hr at room temperature. After washing, the plates were incubated
586 with a 1:10,000 dilution of goat anti-human IgG-Fc Antibody HRP (Bethyl, A80-104P)
587 for 1hr at room temperature. For detection SureBlue Substrate solution (Seracare,
588 Milford, MA) was added to the washed plates. The reaction was stopped by adding
589 TMB Stop Solution (Seracare, Milford, MA) after 6min to the assay plates. The optical
590 density (O.D.) were read at 450nm. The serum concentration was interpolated from

591 the standard curve using a sigmoidal four parameter logistic curve fit for log of the
592 concentration.

593

594 **Statistical analysis.** One-way non-parametric ANOVA (Kruskall-Wallis) with Dunn's
595 post test for multiple comparisons was performed using GraphPad Prism 8.3.

596

597 **References:**

- 598 1 Wu, N. C. & Wilson, I. A. Structural insights into the design of novel anti-influenza therapies.
599 *Nat Struct Mol Biol* **25**, 115-121, doi:10.1038/s41594-018-0025-9 (2018).
- 600 2 Krammer, F. *et al.* NAction! How Can Neuraminidase-Based Immunity Contribute to Better
601 Influenza Virus Vaccines? *mBio* **9**, doi:10.1128/mBio.02332-17 (2018).
- 602 3 Corti, D. *et al.* A neutralizing antibody selected from plasma cells that binds to group 1 and
603 group 2 influenza A hemagglutinins. *Science* **333**, 850-856, doi:10.1126/science.1205669
604 (2011).
- 605 4 Dreyfus, C. *et al.* Highly conserved protective epitopes on influenza B viruses. *Science* **337**,
606 1343-1348, doi:10.1126/science.1222908 (2012).
- 607 5 Ekiert, D. C. *et al.* Antibody recognition of a highly conserved influenza virus epitope. *Science*
608 **324**, 246-251, doi:10.1126/science.1171491 (2009).
- 609 6 Ekiert, D. C. *et al.* A highly conserved neutralizing epitope on group 2 influenza A viruses.
610 *Science* **333**, 843-850, doi:10.1126/science.1204839 (2011).
- 611 7 Kallewaard, N. L. *et al.* Structure and Function Analysis of an Antibody Recognizing All
612 Influenza A Subtypes. *Cell* **166**, 596-608, doi:10.1016/j.cell.2016.05.073 (2016).
- 613 8 Bangaru, S. *et al.* A Site of Vulnerability on the Influenza Virus Hemagglutinin Head Domain
614 Trimer Interface. *Cell* **177**, 1136-1152.e1118, doi:10.1016/j.cell.2019.04.011 (2019).
- 615 9 Ekiert, D. C. *et al.* Cross-neutralization of influenza A viruses mediated by a single antibody
616 loop. *Nature* **489**, 526-532, doi:10.1038/nature11414 (2012).
- 617 10 Rijal, P. *et al.* Broadly inhibiting anti-neuraminidase monoclonal antibodies induced by
618 trivalent influenza vaccine and H7N9 infection in humans. *J Virol*, doi:10.1128/jvi.01182-19
619 (2019).
- 620 11 Ali, S. O. *et al.* Evaluation of MEDI8852, an Anti-Influenza A Monoclonal Antibody, in Treating
621 Acute Uncomplicated Influenza. *Antimicrob Agents Chemother* **62**, doi:10.1128/aac.00694-
622 18 (2018).

- 623 12 Deng, R. *et al.* Pharmacokinetics of MHAA4549A, an Anti-Influenza A Monoclonal Antibody,
624 in Healthy Subjects Challenged with Influenza A Virus in a Phase IIa Randomized Trial. *Clin*
625 *Pharmacokinet* **57**, 367-377, doi:10.1007/s40262-017-0564-y (2018).
- 626 13 Hershberger, E. *et al.* Safety and efficacy of monoclonal antibody VIS410 in adults with
627 uncomplicated influenza A infection: Results from a randomized, double-blind, phase-2,
628 placebo-controlled study. *EBioMedicine* **40**, 574-582, doi:10.1016/j.ebiom.2018.12.051
629 (2019).
- 630 14 Sparrow, E., Friede, M., Sheikh, M., Torvaldsen, S. & Newall, A. T. Passive immunization for
631 influenza through antibody therapies, a review of the pipeline, challenges and potential
632 applications. *Vaccine* **34**, 5442-5448, doi:10.1016/j.vaccine.2016.08.057 (2016).
- 633 15 Janke, B. H. Influenza A virus infections in swine: pathogenesis and diagnosis. *Vet Pathol* **51**,
634 410-426, doi:10.1177/0300985813513043 (2014).
- 635 16 Rajao, D. S. & Vincent, A. L. Swine as a model for influenza A virus infection and immunity.
636 *ILAR J* **56**, 44-52, doi:10.1093/ilar/ilv002 (2015).
- 637 17 Manam, S. *et al.* Plasmid DNA vaccines: tissue distribution and effects of DNA sequence,
638 adjuvants and delivery method on integration into host DNA. *Intervirology* **43**, 273-281,
639 doi:10.1159/000053994 (2000).
- 640 18 Ledwith, B. J. *et al.* Plasmid DNA vaccines: investigation of integration into host cellular DNA
641 following intramuscular injection in mice. *Intervirology* **43**, 258-272, doi:10.1159/000053993
642 (2000).
- 643 19 Schnepf, B. C., Jensen, R. L., Chen, C. L., Johnson, P. R. & Clark, K. R. Characterization of
644 adeno-associated virus genomes isolated from human tissues. *J Virol* **79**, 14793-14803,
645 doi:10.1128/jvi.79.23.14793-14803.2005 (2005).
- 646 20 Zaiss, A. K. *et al.* Differential activation of innate immune responses by adenovirus and
647 adeno-associated virus vectors. *J Virol* **76**, 4580-4590, doi:10.1128/jvi.76.9.4580-4590.2002
648 (2002).

- 649 21 Schlake, T., Thess, A., Fotin-Mleczek, M. & Kallen, K. J. Developing mRNA-vaccine
650 technologies. *RNA Biol* **9**, 1319-1330, doi:10.4161/rna.22269 (2012).
- 651 22 Kormann, M. S. *et al.* Expression of therapeutic proteins after delivery of chemically
652 modified mRNA in mice. *Nat Biotechnol* **29**, 154-157, doi:10.1038/nbt.1733 (2011).
- 653 23 Tiwari, P. M. *et al.* Engineered mRNA-expressed antibodies prevent respiratory syncytial
654 virus infection. *Nat Commun* **9**, 3999, doi:10.1038/s41467-018-06508-3 (2018).
- 655 24 Esquivel, R. N. *et al.* In Vivo Delivery of a DNA-Encoded Monoclonal Antibody Protects Non-
656 human Primates against Zika Virus. *Mol Ther* **27**, 974-985, doi:10.1016/j.ymthe.2019.03.005
657 (2019).
- 658 25 Patel, A. *et al.* In Vivo Delivery of Synthetic Human DNA-Encoded Monoclonal Antibodies
659 Protect against Ebolavirus Infection in a Mouse Model. *Cell Rep* **25**, 1982-1993.e1984,
660 doi:10.1016/j.celrep.2018.10.062 (2018).
- 661 26 Perales-Puchalt, A. *et al.* DNA-encoded bispecific T cell engagers and antibodies present
662 long-term antitumor activity. *JCI Insight* **4**, doi:10.1172/jci.insight.126086 (2019).
- 663 27 Elliott, S. T. C. *et al.* DMAb inoculation of synthetic cross reactive antibodies protects against
664 lethal influenza A and B infections. *NPJ Vaccines* **2**, 18, doi:10.1038/s41541-017-0020-x
665 (2017).
- 666 28 Morgan, S. B. *et al.* Therapeutic Administration of Broadly Neutralizing F16 Antibody Reveals
667 Lack of Interaction Between Human IgG1 and Pig Fc Receptors. *Front Immunol* **9**, 865,
668 doi:10.3389/fimmu.2018.00865 (2018).
- 669 29 DiLillo, D. J., Tan, G. S., Palese, P. & Ravetch, J. V. Broadly neutralizing hemagglutinin stalk-
670 specific antibodies require FcγR interactions for protection against influenza virus in
671 vivo. *Nat Med* **20**, 143-151, doi:10.1038/nm.3443 (2014).
- 672 30 DiLillo, D. J., Palese, P., Wilson, P. C. & Ravetch, J. V. Broadly neutralizing anti-influenza
673 antibodies require Fc receptor engagement for in vivo protection. *J Clin Invest* **126**, 605-610,
674 doi:10.1172/JCI84428 (2016).

- 675 31 Huang, K. Y. *et al.* Focused antibody response to influenza linked to antigenic drift. *J Clin*
676 *Invest* **125**, 2631-2645, doi:10.1172/jci81104 (2015).
- 677 32 Schommer, N. N. *et al.* Active Immunoprophylaxis and Vaccine Augmentations Mediated by
678 a Novel Plasmid DNA Formulation. *Hum Gene Ther* **30**, 523-533, doi:10.1089/hum.2018.241
679 (2019).
- 680 33 Li, Y. *et al.* Immune history shapes specificity of pandemic H1N1 influenza antibody
681 responses. *J Exp Med* **210**, 1493-1500, doi:10.1084/jem.20130212 (2013).
- 682 34 Egli, J. *et al.* The Binding of Human IgG to Minipig FcγR3 - Implications for Preclinical
683 Assessment of Therapeutic Antibodies. *Pharm Res* **36**, 47, doi:10.1007/s11095-019-2574-y
684 (2019).
- 685 35 Mifsud, E. J., Tai, C. M. & Hurt, A. C. Animal models used to assess influenza antivirals. *Expert*
686 *Opin Drug Discov* **13**, 1131-1139, doi:10.1080/17460441.2018.1540586 (2018).
- 687 36 Hemmink, J. D., Whittaker, C. J. & Shelton, H. A. Animal Models in Influenza Research.
688 *Methods Mol Biol* **1836**, 401-430, doi:10.1007/978-1-4939-8678-1_20 (2018).
- 689 37 Bouvier, N. M. & Lowen, A. C. Animal Models for Influenza Virus Pathogenesis and
690 Transmission. *Viruses* **2**, 1530-1563, doi:10.3390/v20801530 (2010).
- 691 38 Margine, I. & Krammer, F. Animal models for influenza viruses: implications for universal
692 vaccine development. *Pathogens* **3**, 845-874, doi:10.3390/pathogens3040845 (2014).
- 693 39 Memoli, M. J. *et al.* Evaluation of Antihemagglutinin and Antineuraminidase Antibodies as
694 Correlates of Protection in an Influenza A/H1N1 Virus Healthy Human Challenge Model.
695 *mBio* **7**, e00417-00416, doi:10.1128/mBio.00417-16 (2016).
- 696 40 Memoli, M. J. *et al.* Validation of the wild-type influenza A human challenge model
697 H1N1pdMIST: an A(H1N1)pdm09 dose-finding investigational new drug study. *Clin Infect Dis*
698 **60**, 693-702, doi:10.1093/cid/ciu924 (2015).

- 699 41 Roestenberg, M., Hoogerwerf, M. A., Ferreira, D. M., Mordmuller, B. & Yazdanbakhsh, M.
700 Experimental infection of human volunteers. *Lancet Infect Dis* **18**, e312-e322,
701 doi:10.1016/s1473-3099(18)30177-4 (2018).
- 702 42 Halbur, P. G. *et al.* Comparison of the pathogenicity of two US porcine reproductive and
703 respiratory syndrome virus isolates with that of the Lelystad virus. *Veterinary pathology* **32**,
704 648-660, doi:10.1177/030098589503200606 (1995).
- 705 43 Vidana, B. *et al.* Heterogeneous pathological outcomes after experimental pH1N1 influenza
706 infection in ferrets correlate with viral replication and host immune responses in the lung.
707 *Vet Res* **45**, 85, doi:10.1186/s13567-014-0085-8 (2014).
- 708 44 Morgan, S. B. *et al.* Aerosol Delivery of a Candidate Universal Influenza Vaccine Reduces Viral
709 Load in Pigs Challenged with Pandemic H1N1 Virus. *J Immunol* **196**, 5014-5023,
710 doi:10.4049/jimmunol.1502632 (2016).
- 711 45 Gauger, P. C. *et al.* Kinetics of lung lesion development and pro-inflammatory cytokine
712 response in pigs with vaccine-associated enhanced respiratory disease induced by challenge
713 with pandemic (2009) A/H1N1 influenza virus. *Vet Pathol* **49**, 900-912,
714 doi:10.1177/0300985812439724 (2012).
- 715 46 Xiao, Y. *et al.* Deep sequencing of 2009 influenza A/H1N1 virus isolated from volunteer
716 human challenge study participants and natural infections. *Virology* **534**, 96-107,
717 doi:10.1016/j.virol.2019.06.004 (2019).
- 718 47 Kim, D., Paggi, J. M., Park, C., Bennett, C. & Salzberg, S. L. Graph-based genome alignment
719 and genotyping with HISAT2 and HISAT-genotype. *Nat Biotechnol* **37**, 907-915,
720 doi:10.1038/s41587-019-0201-4 (2019).
- 721 48 Li, H. *et al.* The Sequence Alignment/Map format and SAMtools. *Bioinformatics* **25**, 2078-
722 2079, doi:10.1093/bioinformatics/btp352 (2009).

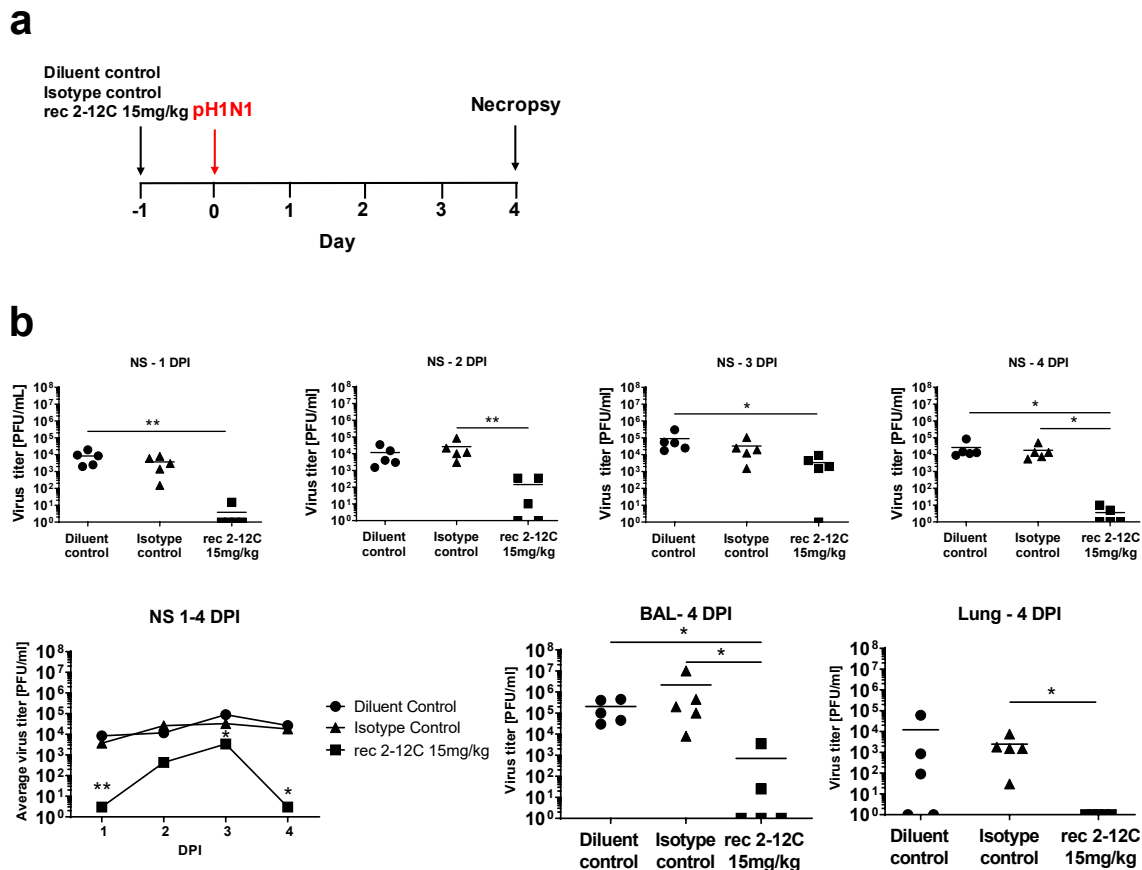
- 723 49 Barbezange, C. *et al.* Seasonal Genetic Drift of Human Influenza A Virus Quasispecies
724 Revealed by Deep Sequencing. *Front Microbiol* **9**, 2596, doi:10.3389/fmicb.2018.02596
725 (2018).
- 726 50 McGinnis, J., Laplante, J., Shudt, M. & George, K. S. Next generation sequencing for whole
727 genome analysis and surveillance of influenza A viruses. *J Clin Virol* **79**, 44-50,
728 doi:10.1016/j.jcv.2016.03.005 (2016).
- 729 51 Xiao, Y. L. *et al.* Deep Sequencing of H7N9 Influenza A Viruses from 16 Infected Patients from
730 2013 to 2015 in Shanghai Reveals Genetic Diversity and Antigenic Drift. *mSphere* **3**,
731 doi:10.1128/mSphereDirect.00462-18 (2018).
- 732 52 Powell, T. J., Silk, J. D., Sharps, J., Fodor, E. & Townsend, A. R. Pseudotyped influenza A virus
733 as a vaccine for the induction of heterotypic immunity. *J Virol* **86**, 13397-13406,
734 doi:10.1128/JVI.01820-12 (2012).
- 735

736 **Acknowledgements.** We are grateful to the animal staff at APHA for excellent
737 animal care and for providing the challenge swine A/Sw/Eng/ 1353/09 influenza virus
738 strain (DEFRA SwIV surveillance programme SW3401). We thank Carlo Bianco from
739 APHA for his support in the image analysis. This work was supported by Bill &
740 Melinda Gates Foundation Grant OPP1201470 and Biotechnology and Biological
741 Sciences Research Council (BBSRC) Grant BBS/E/I/ 00007031. This work was
742 supported in part by the Intramural Research Program of the National Institute of
743 Allergy and Infectious Diseases, National Institutes of Health (YX, JCK, JKT).
744

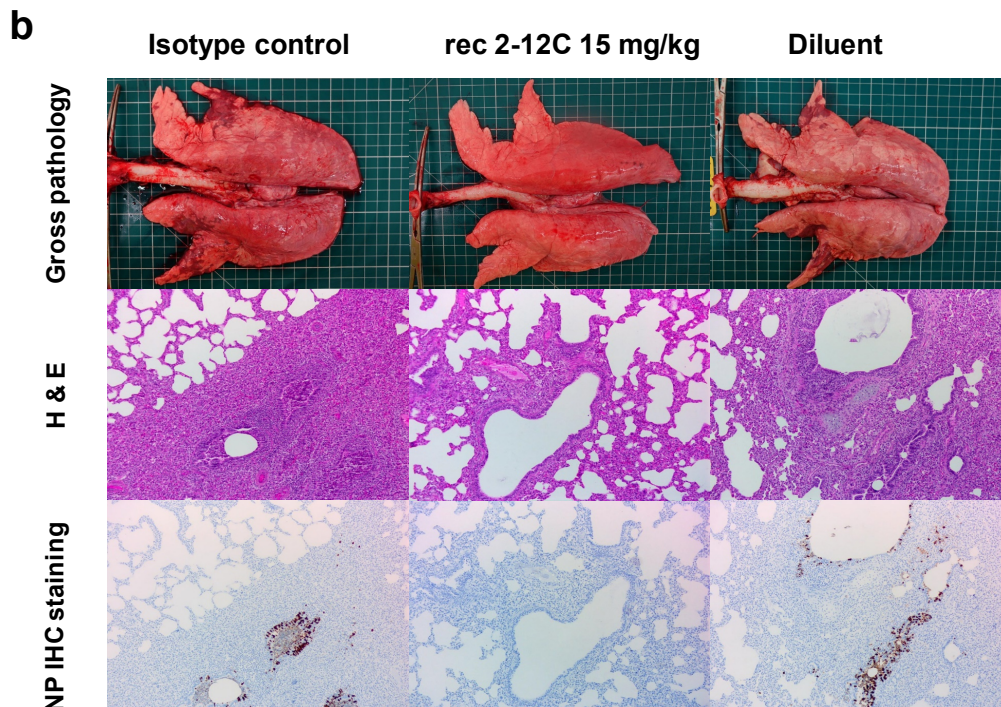
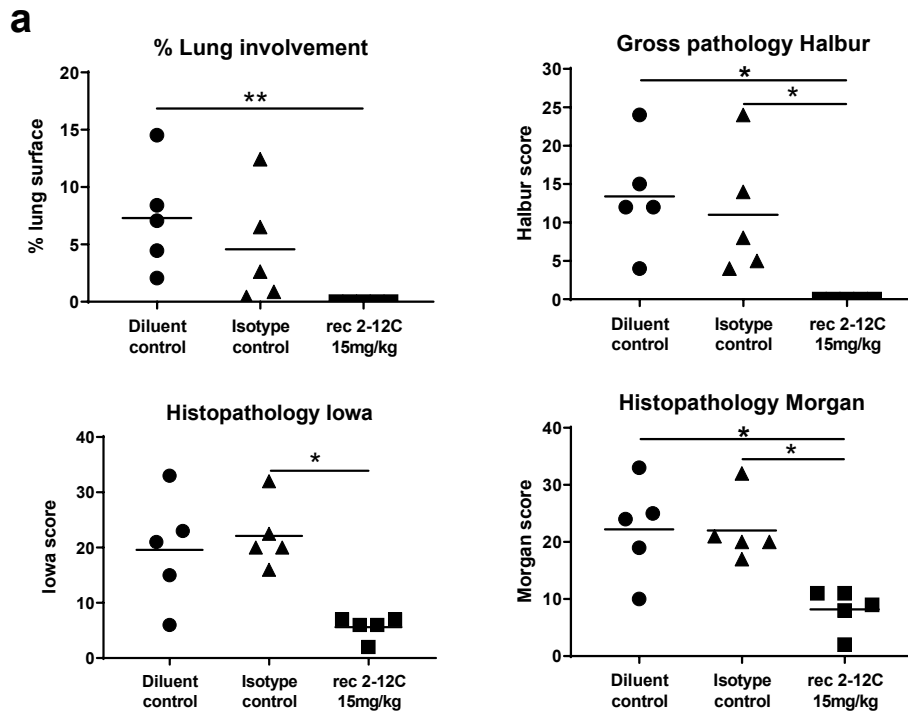
745 **Author contributions:** ET, AM, BH, KB, DW, TS conceived, designed and
746 coordinated the study. ET, AM, BH, BC, EB, GG, HB, KS, SR, PF, AP and SE
747 performed animal experiments, processed samples and analyzed the data. VM, TC,
748 AN and MB carried out post mortem and pathological analyses. YX, JK and JT
749 performed sequencing analysis. ET, AM, PB, TS, KB wrote and revised the manuscript
750 and figures. AT and PR provided reagents and performed microneutralization assays.
751

752 **Conflict of interests:** TS, GB, HB, KS, PF, SR and KB are employees of Inovio
753 Pharmaceuticals and as such receive salary and benefits, including ownership of stock
754 and stock options, from the company. DBW has received grant funding, participates
755 in industry collaborations, has received speaking honoraria, and has received fees for
756 consulting, including serving on scientific review committees and board services.
757 Remuneration received by DW includes direct payments or stock or stock options, and
758 in the interest of disclosure he notes potential conflicts associated with this work with
759 Inovio and possibly others. In addition, he has a patent DNA vaccine delivery pending
760 to Inovio. All other authors report there are no competing interests.

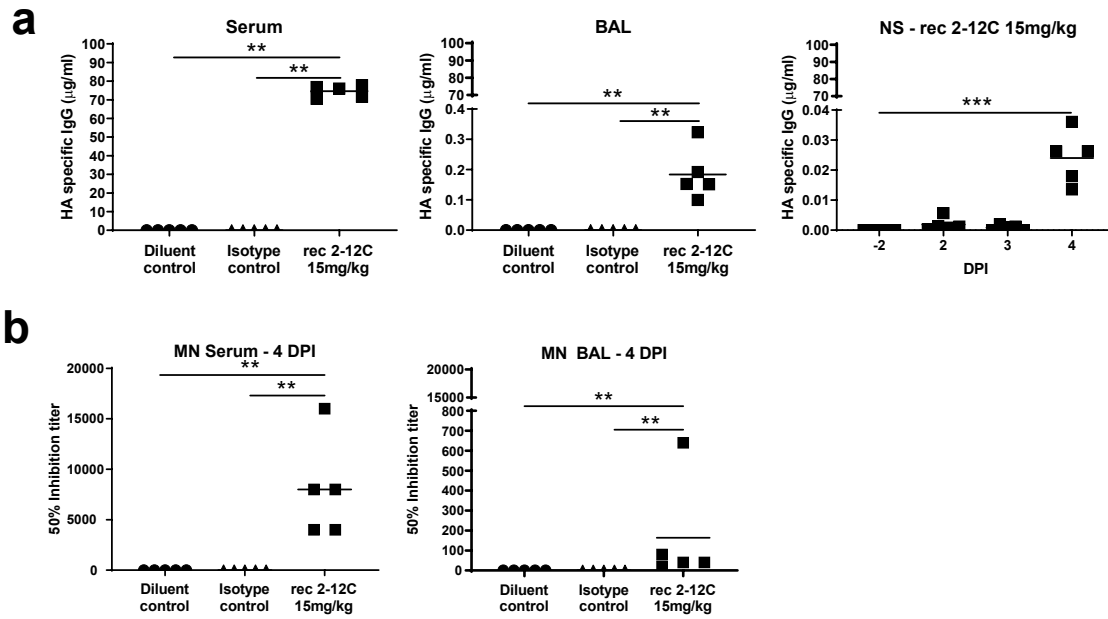
761
762



763
764 **Figure 1. Experimental design and viral load.** Antibodies or diluent were
765 administered intravenously to pigs, which were infected with pH1N1 virus 24 hours
766 later. Nasal swabs (NS) were taken at 1, 2, 3 and 4 days post infection (DPI) and pigs
767 sacrificed at 4 DPI (a). Viral titers in NS, accessory lung lobe (Lung) and BAL at 4DPI
768 were determined by plaque assay (b). Each data point represents an individual pig
769 within the indicated group and bars show the mean. Viral shedding in NS was also
770 represented as the mean of the 5 pigs on each day and significance versus diluent
771 control indicated by asterisks. Viral titers were analysed using one-way non-parametric
772 ANOVA, the Kruskal-Wallis test. Asterisks denote significant differences * $p < 0.05$,
773 ** $p < 0.01$, versus indicated control groups.

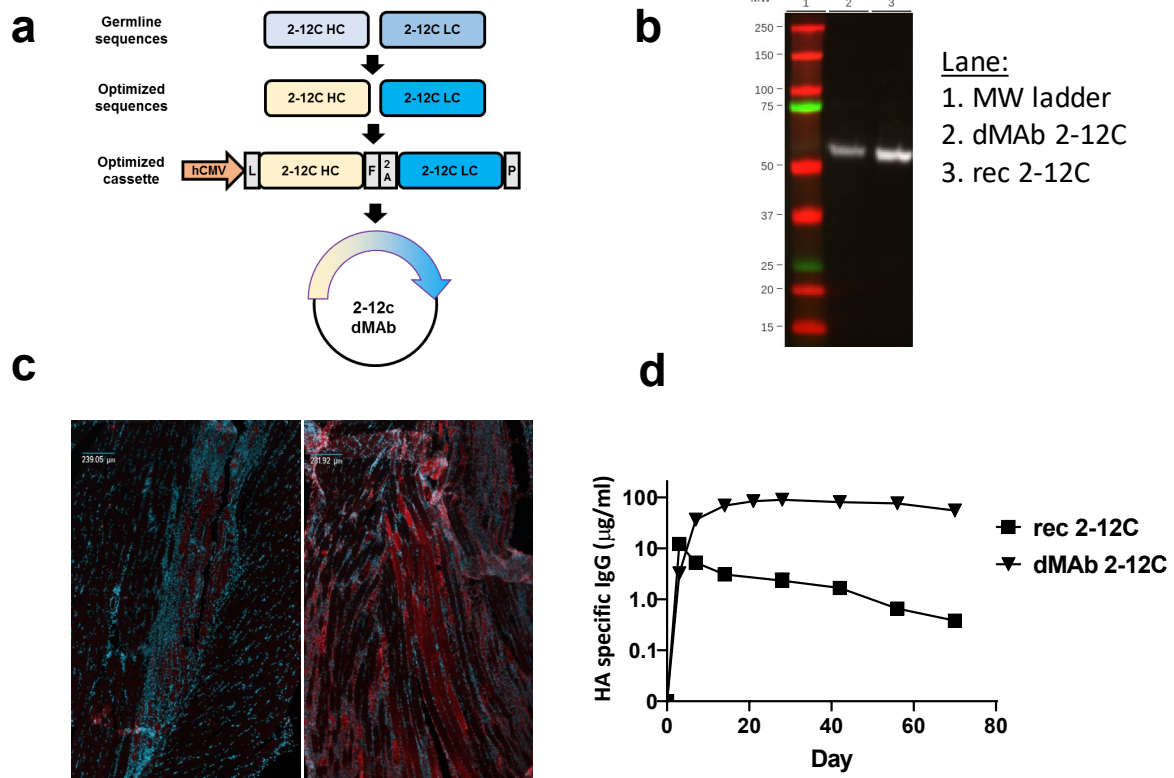


774
 775 **Figure 2. Lung pathology.** Antibodies or diluent were administered intravenously to
 776 pigs, which were infected with pH1N1 virus 24 hours later. The animals were culled at
 777 4 DPI and lungs scored for appearance of gross and histopathological lesions. The
 778 score for each individual in a group and the group means are shown (a).
 779 Representative gross pathology, histopathology (H&E staining; 100x) and
 780 immunohistochemical NP staining (200x) for each group are shown (b). Pathology
 781 scores were analysed using one-way non-parametric ANOVA with the Kruskal-Wallis
 782 test. Asterisks denote significant differences * $p < 0.05$, ** $p < 0.01$, versus indicated
 783 control groups.



784
785

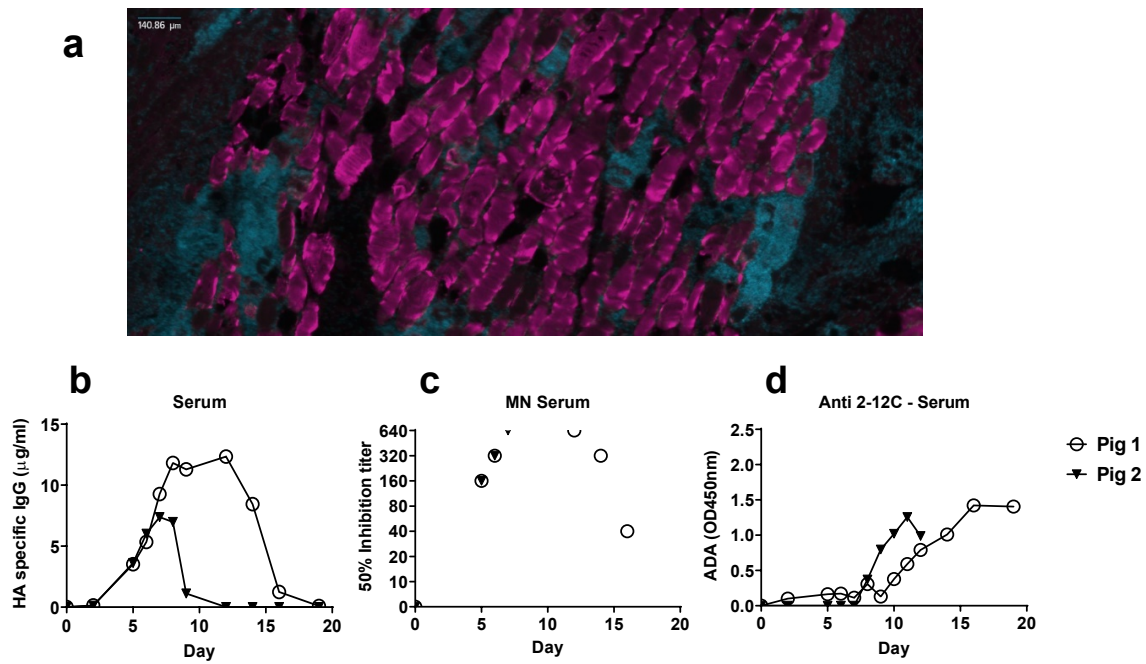
786 **Figure 3. Concentration and neutralising titre of 2-12C in serum and mucosal**
787 **tissues.** H1 HA specific IgG in serum, BAL at 4 DPI and nasal swabs (NS) at the
788 indicated DPI (a). 50% neutralization titers against pH1N1 in the serum and BAL at 4
789 DPI (b). Symbols represent an individual pig within the indicated group and lines the
790 mean. Data were analysed using one-way non-parametric ANOVA with the Kruskal-
791 Wallis test. Asterisks denote significant differences * $p < 0.05$, ** $p < 0.01$ and *** $p < 0.001$,
792 versus indicated control groups.



793
794
795
796
797
798
799
800
801
802
803
804
805
806
807
808

Figure 4. Design and expression of anti-influenza dMAb 2-12c. dMAb 2-12C single construct was designed to express human Ig light and heavy chain sequences codon and RNA-optimized for *in vivo* expression (a). The optimized cassette includes a human CMV promoter (hCMV), a human IgG signal sequence (L), 2-12C HC and LC separated by a furin (F) and P2A cleavage site, and bovine growth hormone polyadenylation signal (P). *In vitro* expression of dMAb 2-12C (b). Supernatant from dMAb 2-12C plasmid transfected 293 T cells was run on a western blot next to recombinant 2-12C mAb. *In vivo* expression of dMAb 2-12C (c, d). dMAb 2-12C or pVAX pDNA was administered intramuscularly by electroporation to BALB/c mice. Immunofluorescence images were taken on muscle tissue sections harvested 3 days after pDNA administration (c). Blue = DAPI, red = human IgG. Serum human IgG levels after day 0 administration of recombinant or dMAb 2-12C in BALB/c mice quantified by ELISA (d).

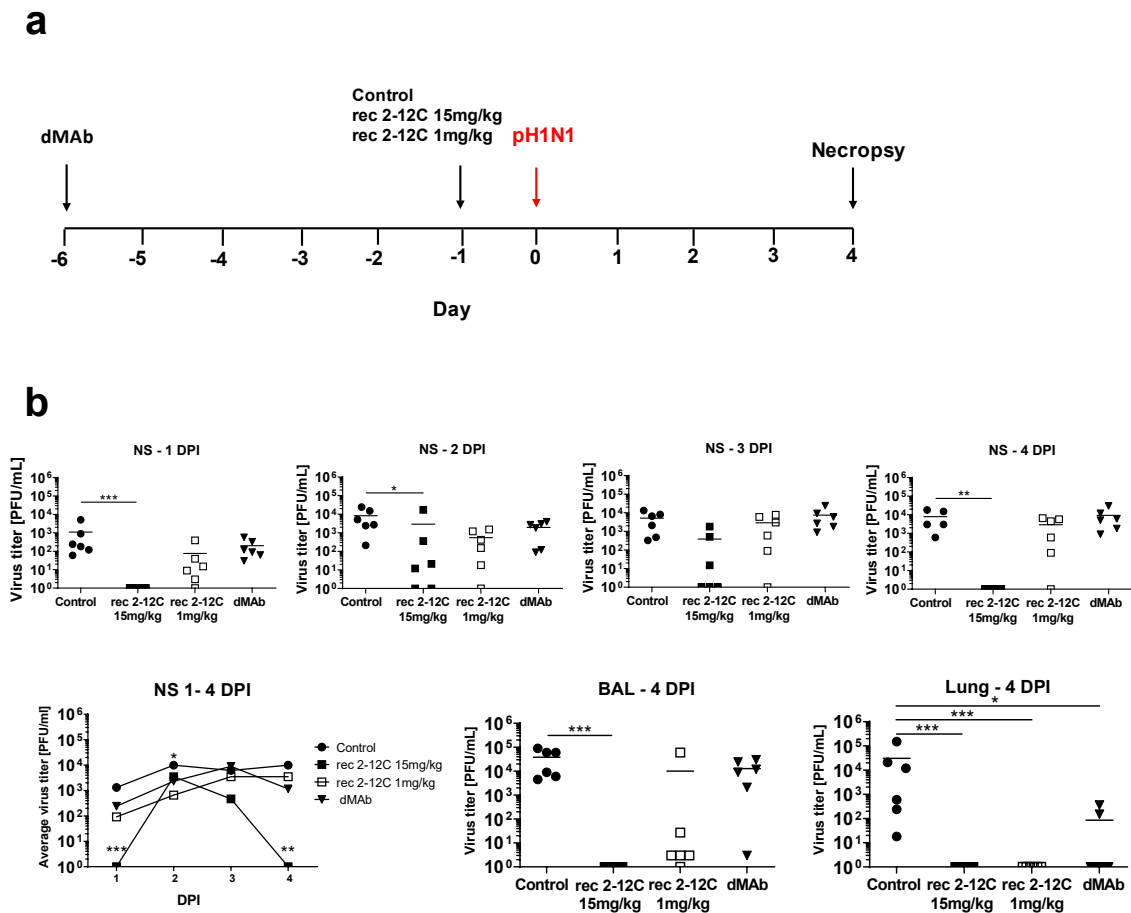
809



810

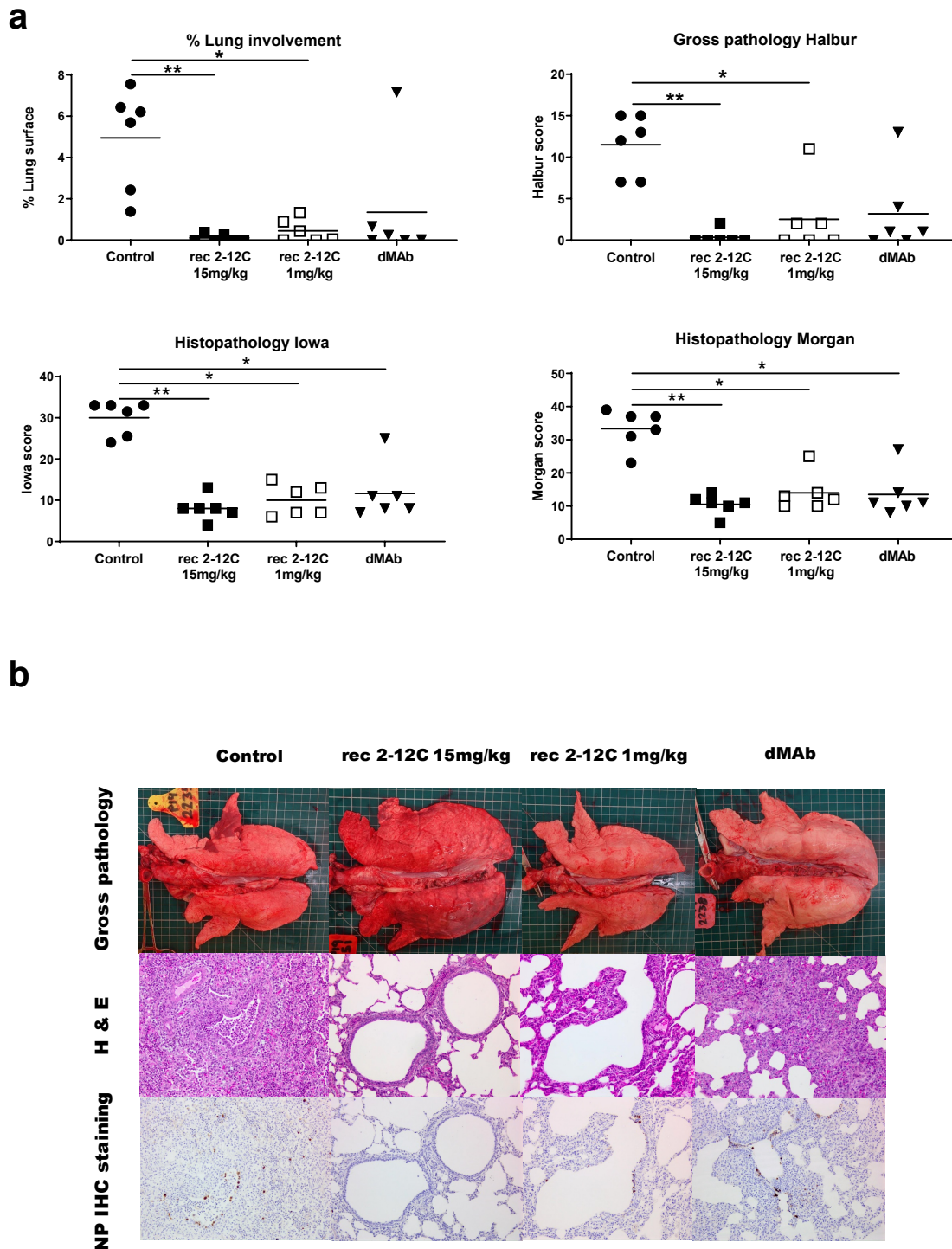
811

812 **Figure 5. Expression of dMAb 2-12C in pigs.** dMAb 2-12C pDNA was administered into the
813 quadriceps muscle of Yorkshire pigs on day 0. Immunofluorescence images were taken on
814 muscle tissue sections harvested 3 days after pDNA administration (a). Blue = DAPI, red =
815 human IgG. Serum 2-12C levels after day 0 administration of dMAb 2-12C were quantified by
816 ELISA (b). Serum neutralizing activity of H1N1 in a microneutralization assay (c). Anti-drug-
817 antibody (ADA) response against 2-12C mAb measured by ELISA (d).



818
819
820
821
822
823
824
825
826
827
828
829
830
831

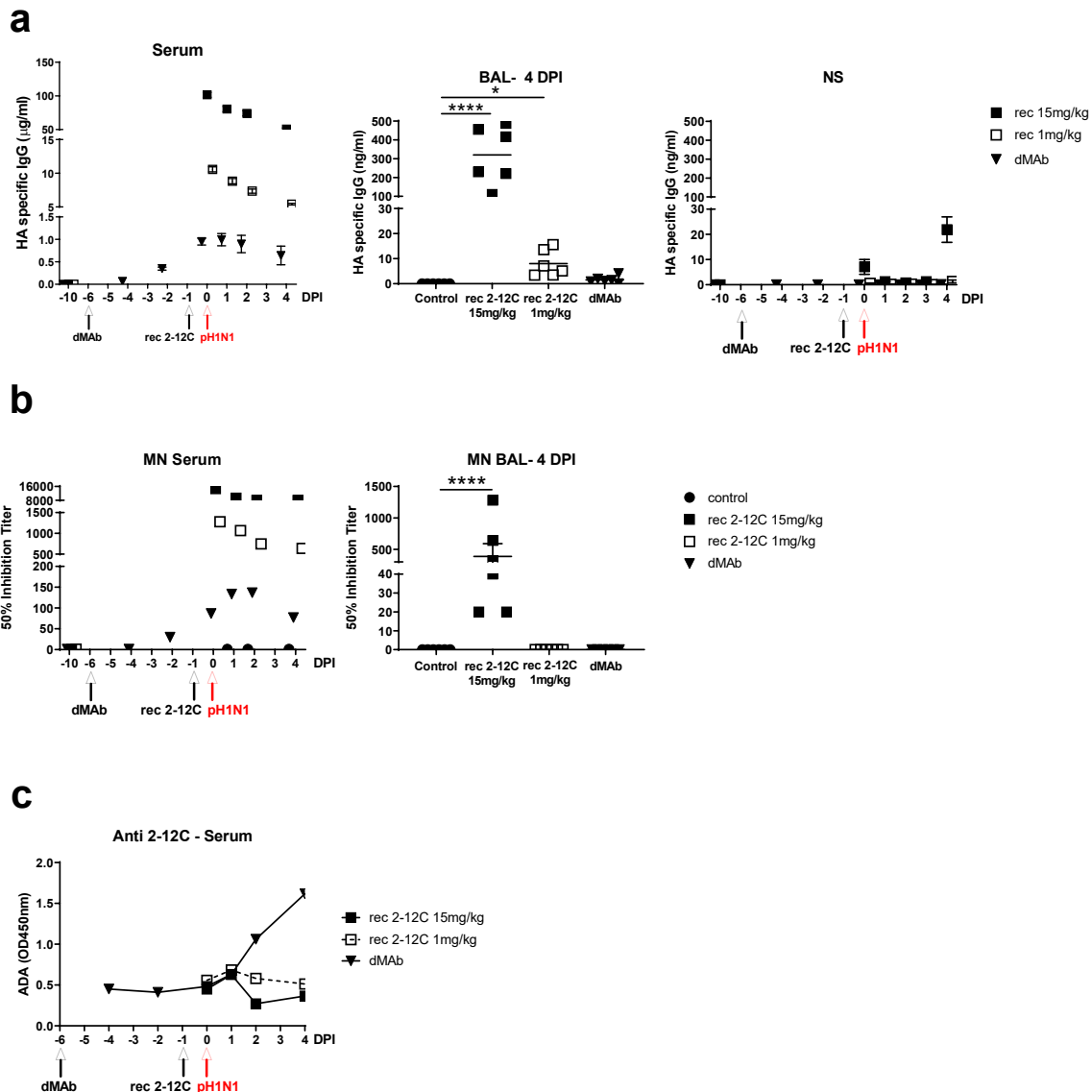
Figure 6: Experimental design and tissue viral load after recombinant and dMAb 2-12C treatment. Six days before pH1N1 challenge 6 mg of dMAb 2-12C was administered intramuscularly by electroporation. Recombinant 2-12C at 15 mg/kg and 1 mg/kg were delivered intravenously 24 hours before challenge. Control group was untreated animals. Nasal swabs (NS) were taken at 0, 1, 2, 3 and 4 DPI and pigs culled at 4 DPI (a). Viral titers in daily NS, BAL and accessory lung lobe (Lung) at 4 DPI were determined by plaque assay (b). Each data point represents an individual within the indicated group and bar is the mean. Viral shedding in NS is also shown as the mean of the 6 pigs over time and significance indicated against the control. Asterisks denote significant differences * $p < 0.05$, ** $p < 0.01$ and *** $p < 0.001$, versus control as analyzed by Kruskal -Wallis test.



832
833
834
835
836
837
838
839
840
841

Figure 7: Lung pathology after recombinant and dMAb 2-12C administration.

Six days before pH1N1 challenge 6 mg dMAb 2-12C was administered intramuscularly by electroporation. Recombinant 2-12C at 15 mg/kg and 1 mg/kg were delivered intravenously 24 hours before challenge. Controls were untreated animals. The animals were culled at 4 DPI and lungs scored for appearance of gross and histopathological lesions (a). Representative gross pathology, histopathology (H&E staining; 200x) and immunohistochemical NP staining (200x) for each group are shown (b). Asterisks denote significant differences *p<0.05, **p<0.01 and ***p<0.001, versus control group as analyzed by Kruskal -Wallis test.



842
843
844
845
846
847
848
849
850
851
852
853

Figure 8: 2-12C levels and anti-viral activity in serum and mucosal tissues after recombinant and dMAb 2-12C administration. The concentration of 2-12C in the serum, BAL and NS was quantified by HA specific ELISA at the indicated time points after administration and pH1N1 challenge (a). The mean 50% neutralization inhibition values for the individual groups in serum over time and BAL at 4 DPI (b). Anti-2-12C antibody (ADA) responses in serum detected by binding to immobilised 2-12C mAb (c). Data were analysed using one-way non-parametric ANOVA with the Kruskal-Wallis test. Asterisks denote significant differences * $p < 0.05$, ** $p < 0.01$ and *** $p < 0.001$, versus control group.

Table 1. SNPs in inoculant virus comparing to A/swine/England/1353/2009

Segment	AA_pos	NT_pos	Ref_base	Coverage	AA_change	SNP_type	A_number	T_number	G_number	C_number	N_number
KR701099.1_NA	454	1361	G	106526	GGT(G)->GTT(V)	nonsyn	A=38(0.000)	T=18689(0.175)	ref=G	C=38(0.000)	N=0(0.000)
KR701097.1_HA	171	511	A	281680	AAA(K)->GAA(E)	nonsyn	ref=A	T=203(0.001)	G=58387(0.207)	C=23(0.000)	N=0(0.000)
KR701097.1_HA	226	676	A	104856	AAG(K)->GAG(E)	nonsyn	ref=A	T=302(0.003)	G=39918(0.381)	C=25(0.000)	N=0(0.000)
KR701096.1_PA	353	1059	G	284452	AAG(K)->AAA(K)	syn	A=41195(0.145)	T=283(0.001)	ref=G	C=60(0.000)	N=0(0.000)
KR701096.1_PA	693	2079	C	109703	TGC(C)->TGT(C)	syn	A=218(0.002)	T=18512(0.169)	G=76(0.001)	ref=C	N=0(0.000)

Amino acid and nucleotide numberings start at Met or ATG.

Table 2. Non-synonymous SNPs in day 3 samples comparing to A/swine/England/1353/2009

Sample	Segment	AA_pos	NT_pos	Ref base	Coverage	AA change	SNP_type	A number	T number	G number	C number	N number	Compare to inoculant
30_naive	KR701097.1_HA	226	676	A	271572	AAG(K)->GAG(E)	nonsyn	ref=A	T=45(0.000)	G=236453(0.871)	C=81(0.000)	N=0(0.000)	Same as inoculant
31_naive	KR701097.1_HA	226	676	A	190623	AAG(K)->GAG(E)	nonsyn	ref=A	T=95(0.000)	G=158242(0.830)	C=43(0.000)	N=0(0.000)	Same as inoculant
51_2-12c	KR701097.1_HA	226	676	A	8398	AAG(K)->GAG(E)	nonsyn	ref=A	T=0(0.000)	G=8394(1.000)	C=0(0.000)	N=0(0.000)	Same as inoculant
53_2-12c	KR701097.1_HA	172	515	G	123369	GGA(G)->GAA(E)	nonsyn	A=14937(0.121)	T=6(0.000)	ref=G	C=22(0.000)	N=0(0.000)	New SNP
	KR701097.1_HA	201	602	C	151699	ACT(T)->ATT(I)	nonsyn	A=14(0.000)	T=16907(0.111)	G=67(0.000)	ref=C	N=0(0.000)	New SNP
	KR701097.1_HA	226	676	A	139973	AAG(K)->GAG(E)	nonsyn	ref=A	T=37(0.000)	G=97706(0.698)	C=54(0.000)	N=0(0.000)	Same as inoculant

Amino acid and nucleotide numberings start at Met or ATG.